ISME

ARTICLE   OPEN

Check for updates

Ecophysiology and genomics of the brackish water adapted SAR11 subclade IIIa

V. Celeste Lanclos [ID]¹, Anna N. Rasmussen², Conner Y. Kojima [ID]¹, Chuankai Cheng¹, Michael W. Henson³, Brant C. Faircloth [ID]⁴, Christopher A. Francis [ID]² and J. Cameron Thrash [ID]¹ ✉

The Order Pelagibacterales (SAR11) is the most abundant group of heterotrophic bacterioplankton in global oceans and comprises multiple subclades with unique spatiotemporal distributions. Subclade IIIa is the primary SAR11 group in brackish waters and shares a common ancestor with the dominant freshwater IIIb (LD12) subclade. Despite its dominance in brackish environments, subclade IIIa lacks systematic genomic or ecological studies. Here, we combine closed genomes from new IIIa isolates, new IIIa MAGS from San Francisco Bay (SFB), and 460 highly complete publicly available SAR11 genomes for the most comprehensive pangenomic study of subclade IIIa to date. Subclade IIIa represents a taxonomic family containing three genera (denoted as subgroups IIIa.1, IIIa.2, and IIIa.3) that had distinct ecological distributions related to salinity. The expansion of taxon selection within subclade IIIa also established previously noted metabolic differentiation in subclade IIIa compared to other SAR11 subclades such as glycine/ serine prototrophy, mosaic glyoxylate shunt presence, and polyhydroxyalkanoate synthesis potential. Our analysis further shows metabolic flexibility among subgroups within IIIa. Additionally, we find that subclade IIIa.3 bridges the marine and freshwater clades based on its potential for compatible solute transport, iron utilization, and bicarbonate management potential. Pure culture experimentation validated differential salinity ranges in IIIa.1 and IIIa.3 and provided detailed IIIa cell size and volume data. This study is an important step forward for understanding the genomic, ecological, and physiological differentiation of subclade IIIa and the overall evolutionary history of SAR11.

INTRODUCTION

The SAR11 clade (Pelagibacterales) is a diverse order of bacterioplankton that constitutes up to 40% of heterotrophic bacteria in surface global oceans [1, 2]. The clade encompasses multiple subclades that exhibit unique spatiotemporal distributions in global waters corresponding to the group's phylogenetic structure [1, 3]. Much of what is known about SAR11 comes from subclade Ia, including the well-characterized strains HTCC1062 and HTCC7211 [4–6]. Studies focused on these organisms and other genomes within Ia defined SAR11 as canonical genome-streamlined oligotrophic marine heterotrophs [7–9] with specific nutrient requirements [10], simple regulatory systems [7, 11, 12], auxotrophies for key amino acids and vitamins [13, 14], partitioning of carbon flow for assimilation or energy based on external nutrient concentrations [15], and sensitivity to purifying selection within closely related populations [16]. Studies of non-Ia SAR11 subclades have provided evidence of additional subclade-specific genomic adaptations and biogeography. For example, subclade Ic contains subtle genomic changes such as amino acid composition, increased intergenic spacer size, and genes encoding for cell wall components as likely adaptations to the bathypelagic [17]. Some subclade II and Ic members possessed genes for nitrate reduction in oxygen minimum zones, providing

the first evidence of facultative anaerobic metabolism in SAR11 [18]. The freshwater LD12/IIIb subclade was recently cultivated and its growth in low brackish salinities and loss of osmoregulation genes provides a hypothesis for SAR11 adaptation into freshwater ecosystems [19, 20].

Another important SAR11 subclade, IIIa, which shares a most recent common ancestor with the freshwater LD12/IIIb group [3, 19] (hereafter LD12), has received comparatively little attention despite being a key group to study the evolutionary transition of SAR11 from marine to fresh water. To date, there are only two reported isolates, HIMB114 (isolated from the Oahu, HI coast [8]) and IMCC9063 (isolated from the Svalbard, Norway coast [21]), but this lack of systematic study is not indicative of IIIa's relevance in global aquatic systems. IIIa is the most abundant SAR11 subclade in brackish waters and its distribution varies based on salinity and phylogenetic position, with two primary branches represented by the two isolates and their genomes [22, 23]. In a survey of the Baltic Sea, the IMCC9063-type of SAR11 was the more abundant representative in brackish waters (salinity < 10) while the HIMB114-type peaked in high-brackish to marine salinities [22]. A similar trend has also been seen across northern Gulf of Mexico estuaries in which multiple operational taxonomic units (OTUs) of SAR11 IIIa were separated ecologically by salinities above and

¹Department of Biological Sciences, University of Southern California, Los Angeles, CA 90089, USA. ²Department of Earth System Science, Stanford University, Stanford, CA 94305, USA. ³Department of Geophysical Sciences, University of Chicago, Chicago, IL 60637, USA. ⁴Department of Biological Sciences and Museum of Natural Science, Louisiana State University, Baton Rouge, LA 70803, USA. ✉email: thrash@usc.edu

below ~10 [23]. In the San Francisco Bay (SFB), a 16S rRNA gene amplicon OTU-based study also found subclade IIIa to dominate at mesohaline salinities [24]. Additionally, the two established branches of IIIa were separated by temperature and latitude in polar versus temperate waters [25]. Despite evidence of niche separation based on their environmental distributions, the temperature and salinity tolerances of these organisms have not been tested experimentally.

There is a comparative paucity of information about subclade IIIa relative to other SAR11, and only limited information has been gleaned from studies using comparative genomics thus far. Neither IIIa representative contains a complete glycolytic pathway, though the neighboring subclade LD12 contains a typical EMP pathway [19] and some subclade I representatives have a variant of the ED pathway [26]. While all SAR11 members are reliant on exogenous reduced sulfur, neither HIMB114 nor IMCC9063 have the genomic potential to use DMSO or DMSP like other SAR11 strains [15, 27–29]. The extensive C1 metabolism found in other SAR11 strains is also lacking in IIIa genomes [17]. Contrary to other well-studied SAR11 members, HIMB114 and IMCC9063 have been reported to contain serABC for glycine/serine prototrophy and IMCC9063 also contains a tenA homolog not found in subclade I that may allow for AmMP rather than HMP to serve as a thiamin source [14]. Together, these genomic predictions suggest that IIIa is fundamentally different from other well-studied SAR11 clades in some aspects of metabolic potential which aligns with the general SAR11 trend of phylogeny reflecting the unique ecology and genomic novelty of particular clades. Furthermore, 16S rRNA gene and phylogenomic trees indicate at least three separate IIIa subgroups instead of only two, raising questions about possible additional genomic and ecological diversification within IIIa [3, 30].

To improve our understanding of the genomic, ecological, and physiological variation present in SAR11 subclade IIIa, we conducted a comprehensive study leveraging new isolates, three closed genomes from these strains, and an additional 468 SAR11 genomes that included new and publicly available metagenome-assembled genomes (MAGs), single-amplified genomes (SAGs), and 1059 metagenomic samples from a variety of aquatic habitats. We examined the pangenomics and global ecology of the group as well as pure culture physiology from two of our isolates. Our results provide strong evidence for three genera within IIIa (IIIa.1, IIIa.2, and IIIa.3) whose ecological distribution is defined at least partially by salinity. We define the genomic adaptations that separate IIIa from the rest of defined clades of SAR11, the three subgroups within IIIa from each other, and partially characterize the physiology and morphology of two isolates from the IIIa branches with cultured representatives. Our SAR11 IIIa strains grown in defined and complex artificial seawater medium, as well as their genomes, provide new opportunities for detailed study of this group.

MATERIALS AND METHODS
Isolation, genome sequencing, and assembly
All strains were isolated using high throughput dilution-to-extinction methods and identified through 16S rRNA gene sequences as previously reported [25, 31]. DNA for strain LSUCC0261 was sequenced using HiSeq (Illumina) after library preparation as previously reported [19] at the Oklahoma Medical Research Facility. DNA for strains LSUCC0664 and LSUCC0723 was sent to the Argonne National Laboratory Environmental Sample Preparation and Sequencing Facility for library preparation and sequencing. We trimmed reads with Trimmomatic v0.36 and assembled trimmed reads for all genomes with SPAdes v3.10.1 [32] using default parameters with coverage cutoff set to "auto". We verified closure of the genomes using Pilon v1.22 [33] and checked the assemblies for contamination using CheckM v1.0.5 [34] with "lineage_wf". See Supplementary Text for detailed methods on isolation, sequencing, assembly, binning, and genome closure verification.

Comparative genomics and genome characteristics
To increase the number of IIIa genomes in our analysis, we assembled MAGs from the San Francisco Bay (SFB) [35] and combed public datasets for highly-complete SAR11 genomes from all subclades using GTDB-Tk [36] as indicated in the Supplementary Methods. Subclades within SAR11 were delineated using phylogenetic branching (Supplementary Text) [37–39], 16S rRNA gene BLAST identity, average nucleotide identity (ANI) [40], and average amino acid identity (AAI) (https://github.com/dparks1134/CompareM, default settings). Comparative genomics was completed using Anvi'o version 7.1 [41, 42] with the pangenomics workflow (https://merenlab.org/2016/11/08/pangenomics-v2) as previously reported [43] using the following annotation sources from Interproscan [44] and anvi-estimate-metabolism: SMART, PRINTS, MobiDBLite, KEGG_Class, KOfam, Gene3D, ProSiteProfiles, SUPERFAMILY, Pfam, CDD, Coils, Hamap, ProSite-Patterns, PANTHER, SFLD, KEGG_Module, PIRSF, and TIGRFAM. Pfam and KOfam were primarily used for detailed gene searches. We searched for bacteriophage in the assembled genomes of LSUCC0261, LSUCC0664, and LSUCC0723 using the Virsorter 'Virome' and 'RefSeq' databases [45]. Lastly, we used CheckM v1.0.5 [34] output values for genome characteristics (coding density, GC%, predicted genes, and estimated genome size) comparison. We estimated the genome size of non-closed genomes from public databases that were at least 80% complete by multiplying the number of base pairs in the genome assembly by the inverse of the estimated completion percentage (Supplementary Table S1).

Competitive metagenomic read recruitment
To examine the distribution of genomes in aquatic systems, we selected 1,059 metagenomes for read recruitment from the following regions and salinity categories: Baltic Sea (oligo-mesohaline) [46, 47], Chesapeake Bay (USA) (fresh-euhaline) [48, 49], Columbia River (USA) (oligo-euhaline) [50], Black Sea (polyhaline) [51], Gulf of Mexico (poly-euhaline) [52], Pearl River (China) (fresh-polyhaline) [53], San Francisco Bay (USA) (fresh-euhaline) [35], BioGeoTraces (euhaline) [54], Tara Oceans (poly-euhaline) [55], and the North Pacific Subtropical Gyre (euhaline) [56] (accession numbers available in Supplementary Table S1). We conducted read mapping and calculation of normalized abundances via Reads Per Kilobase (of genome) per Million (of recruited read base pairs) (RPKM) using RRAP [57].

Growth experiments
To test the salinity and temperature ranges of our isolates, we grew pure cultures in their isolation medium across a range of ionic strengths and temperatures in the dark without shaking. To test for various C, N, and S substrates that could be used by LSUCC0261, we grew the culture in a modified JW2 medium that contained a single carbon, nitrogen, and sulfur source (Supplementary Table S1) in 96×2.1 mL well PTFE plates (Radleys, Essex, UK). Concentrations for the nutrient sources were added to mimic those in the original minimal media as follows: carbon 500 nM, nitrogen 5 µM, sulfur 90 nM for cysteine and methionine, and 500 nM for taurine. After three sequential transfers of the plates every 3–4 weeks, we transferred any wells that showed a cell signature on the flow cytometer to flasks in triplicate with the corresponding C/N/S mixtures and a higher concentration of the carbon substrate (50 µM). All cultures were re-checked for purity after the experiment concluded via Sanger sequencing of the 16S rRNA gene as described [31]. Cell concentrations were enumerated using a Guava EasyCyte 5HT flow cytometer (Millipore, Massachusetts, USA) with previously reported settings [19, 31]. Growth rates were calculated using sparse-growth-curve [58].

Electron microscopy and cell size estimates
LSUCC0261 was grown to 10^6 cells mL^{-1} and 50 mL of culture was fixed with 3% glutaraldehyde at 4 °C overnight. Cells were filtered onto a 0.2 µm Isopore polycarbonate membrane filter (MilliporeSigma) and dehydrated with 20 minute washes at 30%, 40%, 50%, 75%, 80%, 90%, 95%, and 100% ethanol. We used a Tousimis 815 critical point drying system with 100% ethanol. The filters were then placed into a Cressington 108 sputtercoater for 45 s and imaged on the JSM-7001F-LV scanning electron microscope at the University of Southern California Core Center of Excellence in NanoImaging (https://cni.usc.edu). LSUCC0664 was grown to 10^6 cells mL^{-1} and 5 µL of culture was loaded onto a glow discharged 300 mesh carbon filmed grid (EMS:CF300-cu). We removed excess liquid with filter paper after 2 min and stained with 2% uranyl acetate (TED Pella Cat: 19481) for 1 min. The samples were imaged with a JEM-1400 transmission electron microscope at Louisiana State University Shared Instrumentation Facility
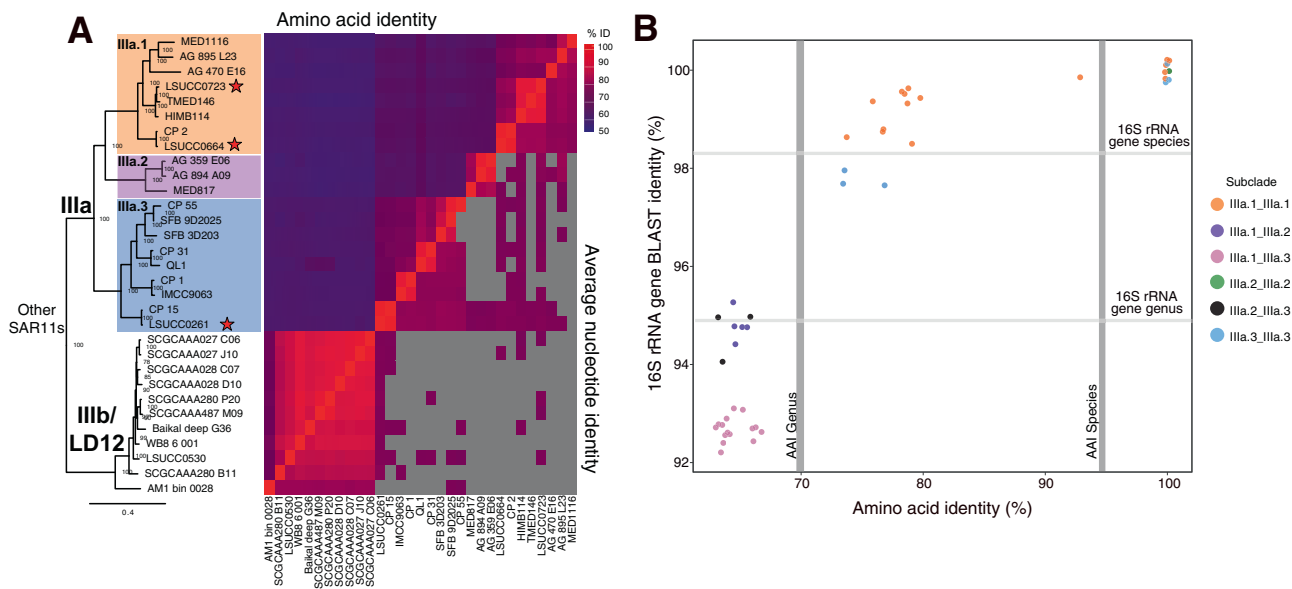
Fig. 1 Subclade structure and genome similarity. A Phylogeny and ANI/AAI pairwise comparison of SAR11 IIIa and IIIb/LD12. The phylogeny is a subset of the phylogenomic tree found in Supplementary Fig. 2. Node values are indicators of bootstrap support ($n = 1000$). Stars indicate new isolates from this analysis. **B** 16S rRNA gene BLAST identity vs AAI. Gray bars indicate the species and genera definitions using AAI [97] and 16S rRNA genes [60] where noted.

Table 1. Genome statistics of new IIIa isolates compared to other SAR11 genomes. Genome size estimates were calculated by multiplying the assembly size by the inverse of the estimated completion from CheckM [34].

Genome	Subclade	Contigs in Assembly	Completion (%)[a]	Est. Contamination (%)	GC (%)	Genome Size (Mbp)[b]	Coding density (%)	Predicted genes
LSUCC0664	IIIa.1	1	100	0	30	1.17	96	1256
LSUCC0723	IIIa.1	1	100	0	29	1.2	96	1309
LSUCC0261	IIIa.3	1	100	0	30	1.27	96	1330
Other IIIa	IIIa	1–122	52.38–99.78	0–5.95	28–32	0.89–1.52	80–97	658–1894
Other SAR11	I,II,LD12	1–288	50.94–100	0–4.67	28–36	0.94–1.75	92–97	654–1788

[a]Completion criteria of >80% for subclade I/II genomes from GTDB-Tk.
[b]Genome size was estimated for incomplete genomes.

(https://www.lsu.edu/sif/). We estimated cell volumes using Pappus' centroid theorem (Supplementary Text).

RESULTS
New isolate genome and MAG characteristics
During the course of previous large-scale culturing experiments, we isolated multiple strains of SAR11 IIIa from the northern Gulf of Mexico [23, 31]. We chose three of these isolates (LSUCC0261, LSUCC0664, and LSUCC0723) for further genomic investigation based on their distribution across the 16S rRNA gene tree within SAR11 IIIa [23]. Genome sequencing and assembly resulted in a single circular contig for each isolate genome. We assembled eight SAR11 genomes from the San Francisco Bay, two of which were subclade IIIa.3 members (Fig. 1A). The two IIIa.3 MAGs generated from SFB were SFB9D2025, which is 0.6 Mb, 52.4% completeness, 5.7% contamination, and was generated from waters with a salinity of 23.6, and SFB3D203, which is 0.9 Mb, 72.6% completeness, 6% contamination, and was generated from waters with a salinity of 5.7. Characteristically of other SAR11 genomes, our isolate genomes and others from IIIa had low GC content (29–30%) and high coding density (96%) (Table 1, Supplementary Fig. S1). However, subclade IIIa joins subclades II

and LD12 as having smaller genomes than those in subclade I (Supplementary Fig. S1).

Phylogenomics, taxonomy, and genome trends
Phylogenomics of 471 SAR11 genomes resolved our isolates as novel members of subclade IIIa (Supplementary Fig. S2), and reproduced the three previously observed IIIa subgroups, delineated as IIIa.1, IIIa.2, and IIIa.3 (Fig. 1A). While a similar nomenclature was recently proposed [30], we have re-classified the subgroups using results from more genomes, amino acid identity (AAI), and 16S rRNA gene identity (Fig. 1B). Both 16S rRNA gene and AAI identities show that IIIa.1 is more similar to IIIa.2 than IIIa.3 (Fig. 1B). The lowest 16S rRNA gene identity within IIIa is 92.1% (Supplementary Table S1). Genomes within a subgroup have values of at least 73% AAI to each other with a dropoff of at least 10% AAI between subgroups, which also indicates each subgroup represents genus level classification using AAI [59] (Fig. 1A, B, Supplementary Table S1). Not all of the genomes within IIIa contained a 16S rRNA gene sequence, but those that did shared >97% 16S rRNA sequence identity within a subgroup. This is near the ~98% sequence identity metric for species [60]. We therefore propose that IIIa represents a taxonomic family consisting of three genera.
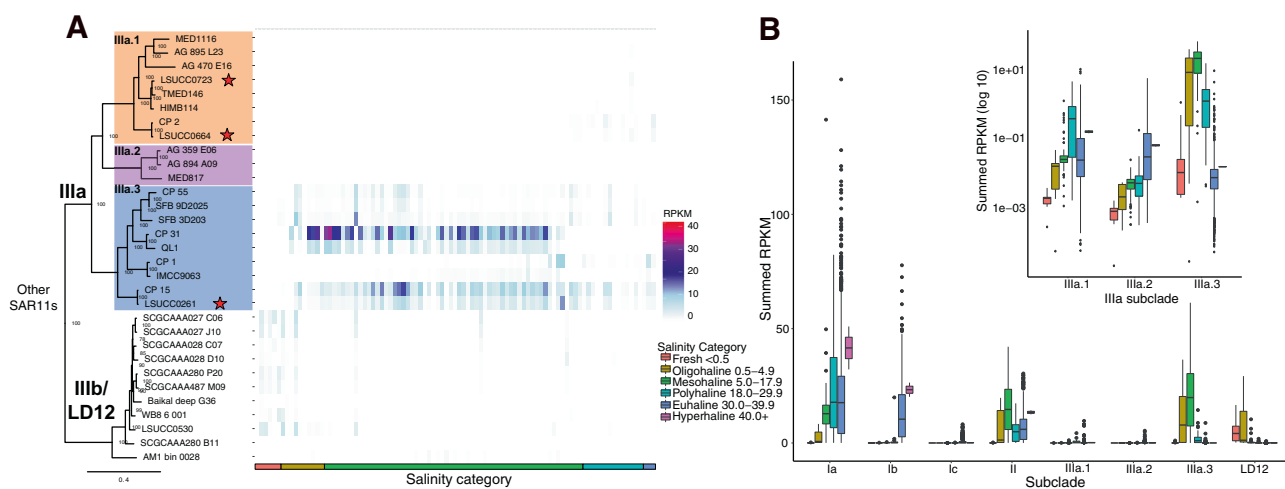
Fig. 2 Distribution of subclade IIIa and LD12 in metagenomic datasets. A Metagenomic recruitment to IIIa and IIIb/LD12 genomes at sites with salinities ≤32. Tiles represent a metagenomic sample that are arranged by increasing salinity on the x-axis. Colors on each tile represent the Reads Per Kilobase (of genome) per Million (of recruited read base pairs) (RPKM) values at the site. Colors on the x-axis indicate the category of salinity the sample belongs to classified by the Venice system [61]. **B** Boxplot of RPKM values summed by subclade for each metagenomic sample grouped by subclade and colored by salinity category. The insert displays log transformed summed RPKM values for subclade IIIa.

Ecological distribution

We recruited reads from 1059 aquatic metagenomes spanning salinities of 0.07–40.2 to 469 SAR11 genomes to evaluate each genome's relative global distribution across marine and estuarine systems (Supplementary Table S1). We categorized salinity following the Venice system (<0.5 fresh, 0.5–4.9 oligohaline, 5–17.9 mesohaline, 18–29.9 polyhaline, 30–39.9 euhaline, > 40 hyperhaline) [61] and summed the RPKM values by subclade within a salinity category for each metagenomic sample. Subclade IIIa overall had a wide ecological distribution with habitat specialization by subgroup (Fig. 2A, B). IIIa.1 was primarily a polyhaline clade with limited recruitment to sites with salinities <18. IIIa.2 was euhaline-adapted with the lowest relative abundances of IIIa. IIIa.1 and IIIa.2 abundances were much lower than that of IIIa.3 generally (Fig. 2B). IIIa.3 was the most abundant IIIa subgroup in salinities <30 and appeared primarily adapted for meso/oligohaline environments (Fig. 2B). Genomes CP31, CP15, LSUCC0261, and QL1 dominated the read recruitment in mesohaline waters and LSUCC0261 was the most abundant isolate genome (Fig. 2A), contrasting with the previous use of IMCC9063 and HIMB114 as representatives of the subclade in metagenomic recruitment datasets [22].

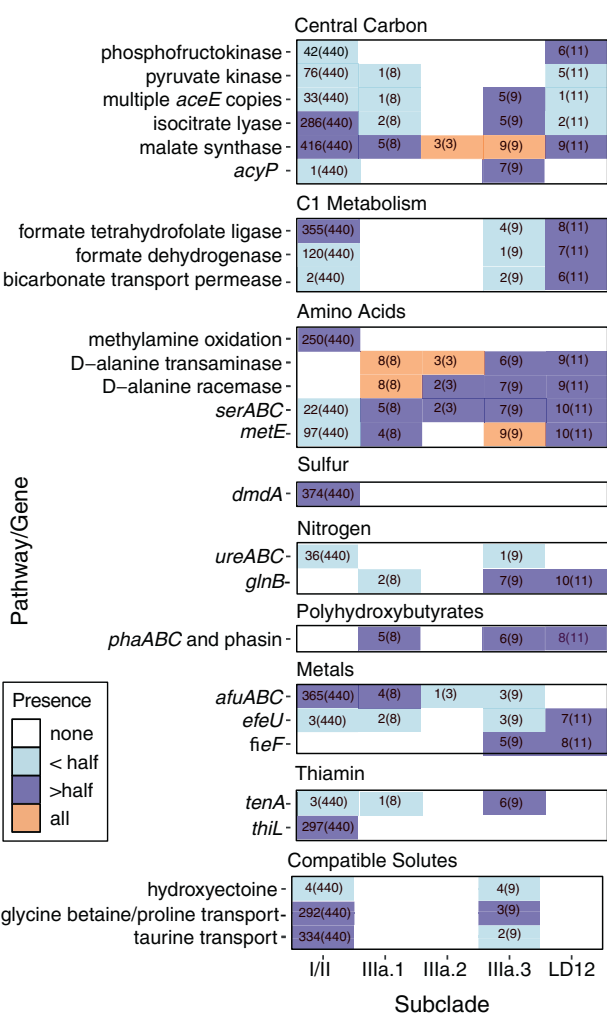## Genomic content of SAR11 IIIa compared to other SAR11

We conducted a pangenomic analysis of all 471 SAR11 genomes to define genome content similarities and differences within IIIa and between IIIa and other SAR11 with the goals of 1) quantifying differences in metabolic potential, and 2) linking genomic variation to different ecological distributions. Our closed isolate genomes and expanded taxon selection within IIIa allowed us to define whether the previously reported genomic content from IMCC9063 and HIMB114 constituted unique or defining traits of their respective subclades. Although SAR11 potentially contains ten subclades [3] or more [30], for our analysis we condensed these into the broad subclades I, II, and LD12, and excluded subclades IV and V since their phylogenetic inclusion within SAR11 is the source of conflicting reports [30, 62–66]. Figure 3 summarizes the genomic differences among SAR11 highlighted below and the complete set of orthologous clusters is in Supplementary Table S1.

Central carbon. IIIa had predicted genes for the pentose phosphate pathway, TCA cycle, and glucose 6-phosphate isomerase like subclades I, II, and LD12. IIIa was missing the EMP glycolysis marker gene, phosphofructokinase, that subclades II and LD12 possessed. Other than one member of IIIa.1, IIIa was also missing the pyruvate kinase commonly found in LD12 and MAGs and SAGs within subclades I and II. IIIa contained pyruvate dehydrogenase (*aceEF*) like subclades I, II, and LD12. Six genomes within IIIa contained at least two copies of *aceE*, with QL1 containing 5 copies. Isocitrate lyase is the first enzyme in the glyoxylate shunt that cleaves isocitrate to glyoxylate and succinate. The glyoxylate shunt was not conserved in IIIa (Fig. 3), as only 2/8 genomes within IIIa.1 and 5/9 genomes in IIIa.3 contained isocitrate lyase, including LSUCC0664 (IIIa.1) and LSUCC0261 (IIIa.3). However, the closed isolate genome of LSUCC0723 (IIIa.1) did not contain a predicted isocitrate lyase, making it the first reported isolate missing this pathway. The second step of the glyoxylate shunt is carried out by malate synthase, which was common in IIIa and all other subclades of SAR11. Subgroup IIIa.3 and a single non-IIIa genome, SCGCAAA240_E13, contained *acyP* that breaks an acyl phosphate into a phosphate, carboxyl group, and a proton.

C1 metabolism. Most IIIa genomes were missing formate-tetrahydrofolate (THF) ligase and formate dehydrogenase for the production of formate and CO_2 from the THF-linked oxidation pathway, except for CP31 (IIIa.3) which had both (Fig. 3). All IIIa genomes lacked the methylamine oxidation genes that were common in I/II SAR11 as previously reported for HIMB114 [8]. Two IIIa.3 genomes, CP31 and LSUCC0261, and six LD12 genomes (including the closed isolate genome LSUCC0530) contained a sodium-dependent bicarbonate transport permease in the SBT protein family. In freshwater and estuarine cyanobacteria, this protein functions as a high affinity bicarbonate transporter that concentrates inorganic carbon within the cell [67]. This probable bicarbonate transporter was found only in CP31 and LSUCC0261 within IIIa.3, which were also two of the genomes that heavily recruited estuary metagenomes (Fig. 2). Though SAR11 is not known to be able to use inorganic carbon for growth, their genomes do contain carbonic anhydrase and anaplerotic enzymes to use inorganic carbon as intermediates in segments of central carbon metabolism [68].

Amino Acids. IIIa and LD12 had the D-alanine transaminase and alanine racemase genes to convert alanine to pyruvate, while other SAR11 did not. Fourteen of twenty genomes from IIIa,

Central Carbon

Pathway/Gene	I/II	IIIa.1	IIIa.2	IIIa.3	LD12
phosphofructokinase	42(440)				6(11)
pyruvate kinase	76(440)	1(8)			5(11)
multiple *aceE* copies	33(440)	1(8)		5(9)	1(11)
isocitrate lyase	286(440)	2(8)		5(9)	2(11)
malate synthase	416(440)	5(8)	3(3)	9(9)	9(11)
acyP	1(440)			7(9)	

C1 Metabolism

Pathway/Gene	I/II	IIIa.1	IIIa.2	IIIa.3	LD12
formate tetrahydrofolate ligase	355(440)			4(9)	8(11)
formate dehydrogenase	120(440)			1(9)	7(11)
bicarbonate transport permease	2(440)			2(9)	6(11)

Amino Acids

Pathway/Gene	I/II	IIIa.1	IIIa.2	IIIa.3	LD12
methylamine oxidation	250(440)				
D–alanine transaminase		8(8)	3(3)	6(9)	9(11)
D–alanine racemase		8(8)	2(3)	7(9)	9(11)
serABC	22(440)	5(8)	2(3)	7(9)	10(11)
metE	97(440)	4(8)		9(9)	10(11)

Sulfur

Pathway/Gene	I/II	IIIa.1	IIIa.2	IIIa.3	LD12
dmdA	374(440)				

Nitrogen

Pathway/Gene	I/II	IIIa.1	IIIa.2	IIIa.3	LD12
ureABC	36(440)			1(9)	
glnB		2(8)		7(9)	10(11)

Polyhydroxybutyrates

Pathway/Gene	I/II	IIIa.1	IIIa.2	IIIa.3	LD12
phaABC and phasin		5(8)		6(9)	8(11)

Metals

Pathway/Gene	I/II	IIIa.1	IIIa.2	IIIa.3	LD12
afuABC	365(440)	4(8)	1(3)	3(9)	
efeU	3(440)	2(8)		3(9)	7(11)
fieF				5(9)	8(11)

Thiamin

Pathway/Gene	I/II	IIIa.1	IIIa.2	IIIa.3	LD12
tenA	3(440)	1(8)		6(9)	
thiL	297(440)				

Compatible Solutes

Pathway/Gene	I/II	IIIa.1	IIIa.2	IIIa.3	LD12
hydroxyectoine	4(440)			4(9)	
glycine betaine/proline transport	292(440)			3(9)	
taurine transport	334(440)			2(9)	

Subclade

Presence
- none
- < half
- > half
- all

Fig. 3 Highlighted comparative gene content in SAR11. Colors and text within the boxes indicate the proportion of genomes in a subclade in which the gene/pathway is present in. Gene suites for ABC transporters or multiple steps in a process are only noted if all components are present while notable pathways missing one component are noted in the text.

including our three isolate genomes, contained *serABC* for the production of serine and glycine from glycolysis. Isolates in subclade I were notedly missing the complete gene suite and were consequently reliant on external glycine and serine for their cellular requirements [10, 13], but our analysis found this gene suite present in some MAGs and SAGs within I/II and LD12 (Fig. 3). IIIa and LD12 also had multiple copies of *metE*, a B12-independent methionine synthase. Though this gene was present in I/II genomes, members of IIIa.3 and LD12 had up to three copies spanning multiple orthologous gene clusters (Supplementary Table S2).

Sulfur. Like all SAR11, IIIa appear dependent on reduced sulfur compounds and contained no complete assimilatory or dissimilatory sulfate reduction pathways [17, 19]. I/II SAR11 were predicted to use DMSO and DMSP, but all IIIa genomes, as well as LD12, were missing *dmdA* for the use of DMSP through the demethylation pathway, confirming the previous observation in the isolate genomes IMCC9063 and HIMB114 [69].

Nitrogen and urease. All SAR11 were predicted to use ammonia and synthesize glutamate and glutamine, though the pathways in which glutamate was synthesized were variable. Almost half of IIIa and most LD12 members had *glnB*, a part of the P-II nitrogen response system frequently found in Proteobacteria that is

missing in other members of SAR11 [12] (Fig. 3). The P-II associated *glnD* gene was not found in any genome, so it is unclear what nitrogen response differences, if any, *glnB* can confer for IIIa/LD12. We found a urease gene suite operon, *ureABC,* and accessory proteins *ureEFGHJ* in the isolate LSUCC0261 (IIIa.3) genome with the nickel/peptide ABC transporter commonly found in SAR11. Functional urease operons require a nickel cofactor [70], so the presence of the urease and accessory proteins just downstream of the ABC transporter indicated a likely functional gene suite, which we confirmed with growth experiments (below). Thirty-six MAGs from subclade I also contained the urease gene suite (Supplementary Table S2). Urease in SAR11 was first reported in the Eastern Tropical North Pacific oxygen deficient zone where up to 10% of SAR11 were reported to contain the genes [71]. Ours is the first reported SAR11 isolate to contain urease and the only extant member of IIIa or LD12 with these genes.

Polyhydroxyalkanoates. We found 11/20 genomes within IIIa.1/ IIIa.3 and 8/11 genomes in LD12 contained *phaABC* and an associated phasin protein for the predicted production and use of polyhydroxybutyrate (or another polyhydroxyalkanoate) (Fig. 3). In other organisms, *phaABC* and phasin proteins allow cells to store carbon intracellularly when carbon is high but another essential component of growth such as nitrogen, phosphorous, magnesium, or oxygen is limiting/unbalanced [72]. These granules also have been noted to protect cells from stressors such as temperature, reactive oxygen species, osmotic shock, oxidative stress, or UV damage [73]. These genes have been reported in limited IIIa.1 genomes previously [74, 75], but we extend this observation to additional isolates and confirm storage granule synthesis potential as a widespread phenomenon in the IIIa and LD12 subclades. Furthermore, this potential phenotype contrasts with the concept of oceanic SAR11 cells storing phosphate in an extracellular buffer [76]. The selection pressure for this gene suite requires further investigation given the broad range of functions for these compounds and the generally high nutrient load of coastal and brackish waters where IIIa and LD12 predominate.

Metals. The Fe^{3+} ABC transporter common in subclade I/II SAR11 was found throughout IIIa. Two IIIa.1, three IIIa.3, and seven LD12 representatives as well as three subclade I/II genomes also contained *efeU*, a high affinity ferrous iron (Fe^{2+}) transporter, and IIIa.3 and LD12 members contained a ferrous-iron (Fe^{2+}) efflux pump *fieF* for iron and zinc removal from cells [77] (Fig. 3). Estuarine systems have been noted to contain significant amounts of available Fe^{2+} [78], so these genes indicate a potential iron availability niche of which some these specialized SAR11 can take advantage.

Compatible solutes. An ectoine permease was found in all SAR11 subclades except for IIIa.2 and LD12, but only IIIa.3 members LSUCC0261, CP15, and CP55 (and four SAGS from other subclades) were predicted to synthesize hydroxyectoine from ectoine (Fig. 3). Hydroxyectoine is a broad-spectrum osmoprotective molecule for cells, can protect cells against desiccation, and its production was increased during stationary phase when grown in high salt stress in a minimal media in halophile *Virgibacillus halodenitrificans* PDB-F2 [79, 80]. The glycine betaine/proline transporter was present throughout IIIa, but IIIa.3 representatives LSUCC0261, CP15, and QL1 were the only members that contain all the subunits, including the ATP binding subunit. This transporter was missing completely in LD12 [19]. IIIa.3 members LSUCC0261 and CP15 were the only members of IIIa that could transport taurine like subclades I/II. IIIa was also missing mannitol synthesis/transport, sorbitol transport, sarcosine synthesis, and TMAO synthesis though these systems are found in some other I/II SAR11. These findings show IIIa contained intermediate numbers of compatible solute genes in between those of I/II and LD12 (Fig. 3). IIIa.3 contained the most compatible solute genes within IIIa.

Vitamins/cofactors and other genomic features. Six IIIa.3 genomes (including the isolates IMCC9063 and LSUCC0261), one
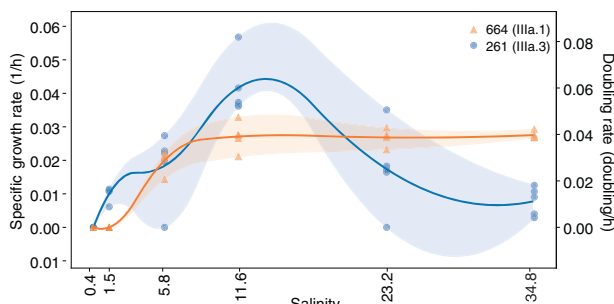
IIIa.1 genome, and three SAGs outside of IIIa contained *tenA* that should allow the cells to use AmMP rather than HMP as a source of thiamin precursor unlike other SAR11 [14], This distinction is interesting because we also verified that the previously reported loss of the *thiL* gene [14] to phosphorylate thiamin monophosphate to the biologically available thiamin diphosphate (TPP) was conserved throughout subclade IIIa. Thus, although IIIa may exhibit some niche differentiation from Ia via import of a different thiamin precursor, how IIIa produces TPP for use in the cell is unresolved (Supplementary Text). Like other SAR11, IIIa had proteorhodopsin–IIIa.1 was a mixture of green and blue (amino acid L/Q at position 105, respectively), IIIa.2 has blue, IIIa.3 has green (Fig. S3, Supplementary Text). These spectral tunings correspond to the ecological distribution and source of the genomes with genomes originating from estuarine systems with mesohaline/polyhaline distributions having green. HIMB114, CP1, and AG_894_A09 contained two copies of proteorhodopsin belonging to two orthologous clusters (Supplementary Table S2)– the implications of which are currently unclear and require further study. Isolates LSUCC0723, LSUCC0664, and LSUCC0261 contained no identifiable bacteriophage signatures according to Virsorter (Supplementary Table S1).

Salinity and temperature growth ranges

We tested the salinity tolerances of two isolates within IIIa, LSUCC0664 (IIIa.1) and LSUCC0261 (IIIa.3), to contextualize the ecological data reported above and understand whether the distribution in ecological data represents the physiological capabilities of the organisms. LSUCC0664 (IIIa.1) grew at salinities of 5.8–34.8 and LSUCC0261 (IIIa.3) grew at salinities of 1.5–34.8, both with an optimum of 11.6. Though the two isolates have an overlapping salinity growth range, LSUCC0261 (IIIa.3) grew faster than LSUCC0664 (IIIa.1) at all salinities except for 23.3 and 34.8, and notably could grow at lower salinities than LSUCC0664 (Fig. 4). These data indicate the IIIa subgroups are euryhaline (capable of inhabiting a wide range of salinities) in distinct contrast with the sister clade LD12 [19]. We also tested isolate LSUCC0261 (IIIa.3) for its temperature range/optimum. It could grow at temperatures of 12–35 °C with its optimum of 30 °C indicating a preference for warmer waters (Supplementary Fig. S4). While rates of growth between 30–35 °C were similar, LSUCC0261 grew to a higher cell density in 30 °C (Supplementary Fig. S4).

Minimal C, N, S requirements

We grew LSUCC0261 (IIIa.3) in minimal artificial seawater media to test the isolate's ability to utilize individual carbon, nitrogen, and sulfur sources with a variety of substrate combinations (Supplementary Figs. S5 and S6, Supplementary Table S1). We tested pyruvate, citrate, ribose, acetate, succinate, and α-ketoglutaric acid as C sources, urea and ammonia as N sources, and cysteine, and methionine as S sources. Oxaloacetic acid, taurine, dextrose, sulfate, DMSO, and DMSP did not support growth. These results

are in line with what was predicted by genomics except for oxaloacetic acid which should have been usable as a carbon source due to the presence of *maeB* and its use in isolate HTCC1062 [10]. Also in contrast to our study, HTCC1062 was able to use taurine but not acetate as replacements for pyruvate [10] indicating multiple physiological differences between the two isolates.
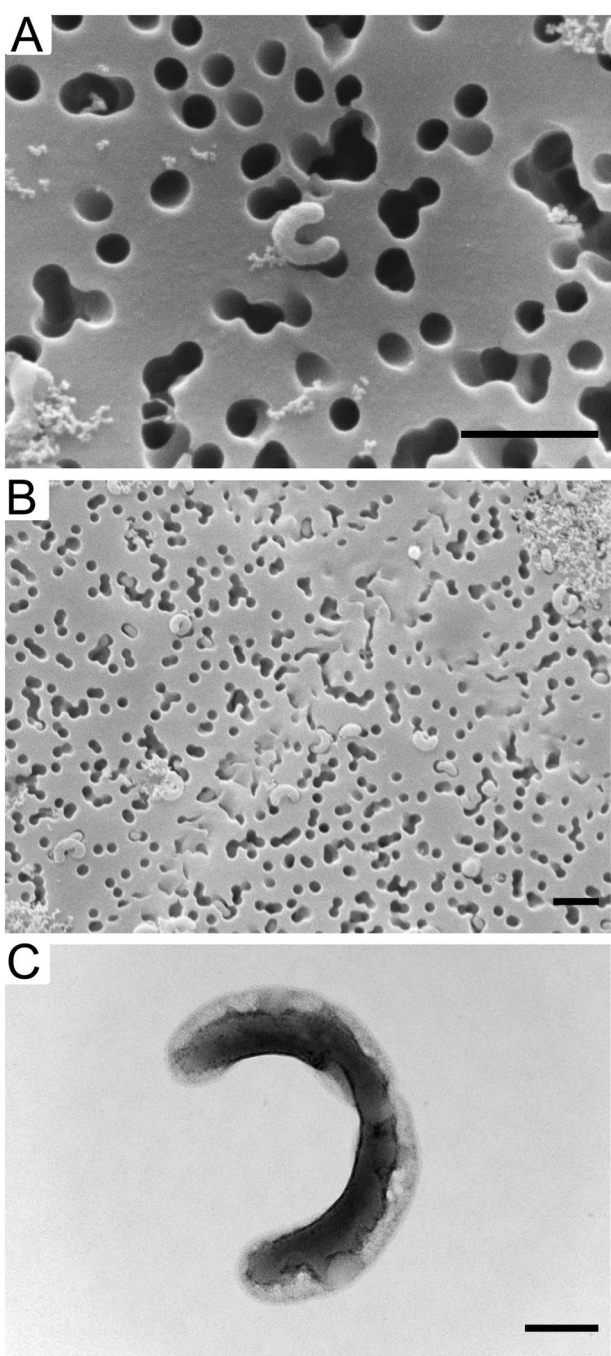
Electron microscopy

Scanning electron microscopy for LSUCC0261 and transmission electron microscopy for LSUCC0664 showed that both cells were curved rods like that of other SAR11 and able to stick inside of the pores of a 0.1 μm laser etched filter (Fig. 5A, B). We estimated the cells at 100–300 nm thick for LSUCC0261 and 150–240 nm thick for LSUCC0664 (Supplementary Fig. S7K), 0.2–1 μm long for LSUCC0261 and 0.4–1.5 μm long for LSUCC0664 (Supplementary Fig. S7L), with volumes between 0.01–0.05 μm^3 for LSUCC0261 and 0.015–0.04 μm^3 for LSUCC0664 (Supplementary Fig. S7M). These values are in line with other estimates of SAR11 [81], thus confirming conserved morphology over large evolutionary distances in the *Pelagibacterales*. These sizes are also notable since SAR11 diameters could allow some cells to pass through traditionally used 0.2 μm filters, while their lengths could result in their collection on filters of 0.8–1 μm, which are sometimes used to separate "particle-attached" taxa. Thus, SAR11 may actually be undersampled in 0.2–1 μm size fraction metagenomes.

DISCUSSION

This study is the first to systematically focus on SAR11 subclade IIIa and constitutes the most current pangenomic study of high-quality publicly available SAR11 genomes and their phylogenetic relationships. We have contributed multiple new pure cultures, their complete genomes, and 2 IIIa MAGs. Previous reports of IIIa genomic content have primarily focused on exceptions to the metabolism of other SAR11 subclades. With our expanded genome selection, we determined whether these findings were conserved features across IIIa or unique to individual isolates. Our study establishes glycine and serine prototrophy, loss of DMSO, DMSP, and much of C1 metabolism, presences of *phaABC* genes, loss of *thiL*, and a mosaic distribution of the glyoxylate shunt as conserved genomic traits within IIIa.

We furthermore confirmed several of these genomic predictions via growth physiology. The isolation of LSUCC0261, LSUCC0664, and LSUCC0723 taxa tested serine and glycine prototrophy because LSUCC0261 was isolated in JW2 medium that does not contain glycine or serine, and LSUCC0664 and LSUCC0723 were isolated in an another medium, MWH2, that did not contain glycine or serine either but did have glycine betaine. HTCC1062 could oxidize glycine betaine as a replacement glycine source [10], but LSUCC0664 and LSUCC0723 do not have the genes to convert glycine betaine to glycine. Thus, the cultivation and propagation of these isolates in our media confirms glycine and serine prototrophy in IIIa. Furthermore, LSUCC0261 did not require glycine or serine in minimal medium experiments (Supplementary Fig. S4) and could not use the reduced sulfur compounds DMSP and DMSO like other SAR11 [28].

This study is the first reported growth of a SAR11 isolate using urea as a sole nitrogen source. Uptake of labeled urea by SAR11 has been observed in situ and the urease can be common in OMZ SAR11 [71]. While we only observed the urease gene suite in one IIIa genome (LSUCC0261), these SAR11 urease genes were found throughout San Francisco Bay water column metagenomes (Supplementary Figs. S8 and S9), suggesting that this metabolism is important for estuarine SAR11. Future work will be needed to determine whether LSUCC0261 uses urea as a source of nitrogen, carbon, or both, explore the frequency of urease in coastal populations, and identify the circumstances by which urease offers a competitive advantage in SAR11.

Fig. 4 Isolate salinity tolerance. Growth rates and doubling times of LSUCC0664 (IIIa.1) in orange and LSUCC0261 (IIIa.3) in blue in media of varying salinities.

Fig. 5 Electron microscopy. A Scanning electron microscopy image of a single LSUCC0261 cell. **B** Scanning electron microscopy image of many LSUCC0261 cells and cellular debris. A-B indicates a 1 μm scale bar. **C** Transmission electron microscopy image of a single LSUCC0664 cell likely mid-division with a scale bar of 200 nm.

Far from being a monolithic subclade with universal features, we propose that subclade IIIa represents a family within the order *Pelagibacterales* and that the subgroups are equivalent to genera defined by both 16S rRNA gene identity and AAI (Fig. 1) [59, 60]. The genera had unique spatio-temporal distributions (Fig. 2B), which aligns with our understanding of the historical delineation of different SAR11 ecotypes [3, 6, 30, 82]. Previous studies defined three phylogenetic branches represented by HIMB114 as a coastal branch (IIIa.1), IMCC9063 (IIIa.3) as a mesohaline branch, and an uncultured oceanic branch between them [3, 22]. Our expanded

taxon selection and comparison to more than a thousand metagenomes refines our understanding of subclade distribution. While IIIa.3 was the most abundant of the subgroups overall, these organisms preferred slightly lower salinities than IIIa.1, and IIIa.2 was primarily a marine group. Such fine-scale salinity differentiation was supported by physiological data. The IIIa.1 isolate LSUCC0664 could not grow at the lowest salinities possible for LSUCC0261 (IIIa.3) (Fig. 4). LSUCC0261 was also best adapted to intermediate salinities, whereas LSUCC0664 grew much better by comparison in higher salinities (Fig. 4).

There is important metabolic diversity between the subgroups within IIIa, with IIIa.3 being the most distinct. Several metabolic traits were unique to IIIa.3 or shared only with the freshwater LD12 clade. In addition to the ability to transport Fe^{3+} via ABC transport as other SAR11, IIIa can use a high affinity ferrous iron (Fe^{2+}) transporter and IIIa.3/LD12 can pump Fe^{2+} and zinc from cells [77]. IIIa.3 contained *acyP* that cleaves acyl-phosphate into a phosphate and carboxylate which may serve as a parallel evolutionary tactic to scavenge phosphate similarly to the methyl phosphonate cleavage in Ia genomes like HTCC7211 [83] or could act simply as an additional way to recycle acetate for the cell's central carbon metabolism. IIIa.3 has the potential for AmMP to fulfill thiamin requirements instead of being reliant on HMP like most other SAR11 [14] due to the presence of *tenA*. In a recent survey of thiamin-related compound concentrations in the North Atlantic, AmMP was found in similar but higher concentrations than HMP at multiple marine stations [84]. This represents a crucial niche-differentiating step for IIIa.3 from other SAR11, including the sister groups IIIa.1 and IIIa.2 that are likely reliant on HMP [14]. Subclade IIIa's conserved deletion of *thiL*, which converts thiamin monophosphate (TP) to the biologically usable thiamin diphosphate (TPP), remains inexplicable as it appears that these organisms still require thiamin diphosphate. For example, eight genomes spanning the three subgroups within IIIa have multiple gene copies of the *aceE* E1 component of pyruvate dehydrogenase and QL1 has five copies. This is notable because gene duplications in SAR11 are limited [8], and also because *aceE* needs thiamin diphosphosphate as a cofactor to combine thiamin diphosphate and pyruvate to make acetyl-CoA [85]. It is thus likely that a currently unannotated gene can complete this final conversion. One possible candidate is an adenylate kinase found in all SAR11 that can convert thiamin diphosphate to thiamin triphosphate [86]. Combined, these notable metabolic shifts in IIIa.3 probably allow for the subclade to exploit environmental resources that other SAR11 are unable to use and contribute to the ecological success of the group relative to the other groups in IIIa.

Authentic estuarine-adapted taxa are believed to be rare compared to marine and freshwater versions [87]. Prior research from river outlets debated whether estuarine-adapted lineages could truly exist or whether the community members in estuarine zones are simply a mixture of freshwater and marine communities because the short residence times of estuarine water make an established community unlikely [88]. However, a genuine brackish community in the Baltic Sea between salinities of 5–8 was distinct from fresh and salty community members [89]. The physiology, ecological distribution, gene content, and sister position of IIIa to LD12 all support the concept of an estuarine origin of the last common ancestor for IIIa/LD12. Subsequently, one subgroup of IIIa remained estuarine-adapted (IIIa.3), whereas the other subgroups diversified into increasingly higher salinity niches over time (IIIa.1 and IIIa.2). Such marine-freshwater transitions in bacterial lineage evolution are rare [90], although we are finding more examples as more data becomes available [91]. Bacteria such as the Methylophilaceae have recently been documented to have freshwater origins for marine relatives [92] and some diatoms such as the Thalassiosirales have extensive marine to freshwater transitions followed by subsequent marine transitions [93]. While IIIa appears to be a transitionary clade diversifying from estuarine

waters back to marine systems, more genomes and further research into physiology and biogeography are needed to improve our understanding of the evolutionary origins and trajectory of this group.

More generally, subclade IIIa represents an intermediate group in the SAR11 evolutionary transition from marine to fresh water. These organisms inhabit a wide range of salinities but are brackish water specialists and share a most recent common ancestor with the exclusively fresh and low-brackish water subclade LD12. The last common ancestor of all SAR11 is believed to be a streamlined marine organism [94], and we currently hypothesize that a key evolutionary step that allowed the colonization of fresh water occurred through the loss of osmolyte transport genes (for glycine-betaine, proline, ectoine, and hydroxyectoine) in the LD12 branch [19]. The tradeoff for this gene loss was that LD12 was prevented from reinhabiting salty waters [19]. We can use the knowledge of subclade IIIa gained from this study to speculate on the driver of this evolutionary transition further. The two isolates, LSUCC0261 and LSUCC0664, have a euryhaline growth range. While this is noteworthy by itself, it is perhaps more important that LSUCC0261 could not grow in the lowest salinity media tested, i.e., fresh water. What prevents this growth at the freshest salinities remains an important question. Key features of SAR11 are small streamlined genomes that have a comparative dearth of regulatory capability [9] and a high number of constitutively expressed genes [95]. A likely scenario is that IIIa constitutive expression of osmolyte transporter genes prevents these taxa from inhabiting fresh water such that their loss let LD12 lineages complete the transition from low brackish to truly freshwater taxa. We are currently investigating this hypothesis with isolates from IIIa and LD12. While the evolutionary trajectory for LD12 may pass through the common ancestor of IIIa and LD12 as outlined above, there is accumulating evidence that the ostensibly exclusively marine SAR11 groups may also colonize freshwater environments either sporadically, at very low abundances, or both [91, 96].

Overall, this study represents the most complete analysis of SAR11 IIIa thus far and is a necessary steppingstone in the understanding of SAR11 IIIa, its role in estuarine systems, and its intermediate place in the evolution of SAR11 from marine to freshwater environments. Future work on IIIa is needed to contextualize functions of noted gene losses and gains, the mode in which IIIa interacts with thiamin derivatives, and the extent at which IIIa members interact with nutrient dynamics in estuaries including urea and production of polyhydroxyalkanoates.

DATA AVAILABILITY
New genomes added from this study are available on FigShare at (https://doi.org/10.6084/m9.figshare.21350343). Assembled isolate genomes for LSUCC0261, LSUCC0664, and LSUCC0723 are available on IMG under Genome IDs 2728369215, 2770939455, and 2739368061, respectively. Raw isolate genome reads are available on NCBI under accession PRJNA864866. Metagenome assembled genomes from the San Francisco Bay are available on NCBI under BioSample accessions SAMN30106608-SAMN30106615. The accessory datasheets from this publication including the pangenome summary are hosted through FigShare (https://figshare.com/projects/Ecophysiology_and_genomics_of_the_brackish_water_adapted_SAR11_subclade_IIIa/144939). Cryostocks of isolates used in this analysis are available upon request.

REFERENCES
1. Schattenhofer M, Fuchs BM, Amann R, Zubkov MV, Tarran GA, Pernthaler J. Latitudinal distribution of prokaryotic picoplankton populations in the Atlantic Ocean. Environ Microbiol. 2009;11:2078–93.
2. Morris RM, Frazar CD, Carlson CA. Basin-scale patterns in the abundance of SAR11 subclades, marine Actinobacteria (OM1), members of the Roseobacter clade and OCS116 in the South Atlantic. Environ Microbiol. 2012;14:1133–44.
3. Vergin KL, Beszteri B, Monier A, Thrash JC, Temperton B, Treusch AH, et al. High-resolution SAR11 ecotype dynamics at the Bermuda Atlantic Time-series study site by phylogenetic placement of pyrosequences. ISME J. 2013;7:1322–32.
4. Stingl U, Tripp HJ, Giovannoni SJ. Improvements of high-throughput culturing yielded novel SAR11 strains and other abundant marine bacteria from the Oregon coast and the Bermuda Atlantic Time Series study site. ISME J. 2007;1:361–71.
5. Rappé MS, Connon SA, Vergin KL, Giovannoni SJ. Cultivation of the ubiquitous SAR11 marine bacterioplankton clade. Nature. 2002;418:630–3.
6. Giovannoni SJ. SAR11 bacteria: the most abundant plankton in the oceans. Ann Rev Mar Sci. 2017;9:231–55.
7. Giovannoni SJ, Tripp HJ, Givan S, Podar M, Vergin KL, Baptista D, et al. Genome streamlining in a cosmopolitan oceanic bacterium. Science. 2005;309:1242–5.
8. Grote J, Thrash JC, Huggett MJ. Streamlining and Core Genome Conservation among highly divergent members of the SAR11 clade. mBio. 2012;3:1–13.
9. Giovannoni SJ, Cameron Thrash J, Temperton B. Implications of streamlining theory for microbial ecology. ISME J. 2014;8:1553–65.
10. Carini P, Steindler L, Beszteri S, Giovannoni SJ. Nutrient requirements for growth of the extreme oligotroph 'Candidatus Pelagibacter ubique' HTCC1062 on a defined medium. ISME J. 2013;7:592–602.
11. Smith DP, Kitner JB, Norbeck AD, Clauss TR, Lipton MS, Michael S, et al. Transcriptional and translational regulatory responses to iron limitation in the globally distributed marine bacterium Candidatus Pelagibacter ubique. PLoS One. 2010;5:e10487.
12. Smith DP, Thrash JC, Nicora CD, Lipton MS, Burnum-Johnson KE, Carini P, et al. Proteomic and transcriptomic analysis of "Candidatus Pelagibacter ubique" describe the first P II-independent response to nitrogen limitation in a free-living Alphaproteobacterium. MBio. 2013;4:1–11.
13. Tripp HJ, Schwalbach MS, Meyer MM, Kitner JB, Breaker RR, Giovannoni SJ. Unique glycine-activated riboswitch linked to glycine-serine auxotrophy in SAR11. Environ Microbiol. 2009;11:230–8.
14. Carini P, Campbell EO, Morré J, Sañudo-Wilhelmy SA, Cameron Thrash J, Bennett SE, et al. Discovery of a SAR11 growth requirement for thiamin's pyrimidine precursor and its distribution in the Sargasso Sea. ISME J. 2014;8:1727–38.
15. Sun J, Steindler L, Thrash JC, Halsey KH, Smith DP, Carter AE, et al. One carbon metabolism in SAR11 pelagic marine bacteria. PLoS One. 2011;6:e23973.
16. Delmont TO, Kiefl E, Kilinc O, Esen OC, Uysal I, Rappé MS, et al. Single-amino acid variants reveal evolutionary processes that shape the biogeography of a global SAR11 subclade. eLIFE. 2019;8:e46497.
17. Thrash JC, Temperton B, Swan BK, Landry ZC, Woyke T, DeLong EF, et al. Single-cell enabled comparative genomics of a deep ocean SAR11 bathytype. ISME J. 2014;8:1440–51.
18. Tsementzi D, Wu J, Deutsch S, Nath S, Rodriguez-R LM, Burns AS, et al. SAR11 bacteria linked to ocean anoxia and nitrogen loss. Nature. 2016;536:179–83.
19. Henson MW, Lanclos VC, Faircloth BC, Thrash JC. Cultivation and genomics of the first freshwater SAR11 (LD12) isolate. ISME J. 2018;12:1846–60.
20. Tsementzi D, Rodriguez-R LM, Ruiz-Perez CA, Meziti A, Hatt JK, Konstantinidis KT. Ecogenomic characterization of widespread, closely-related SAR11 clades of the freshwater genus "Candidatus Fonsibacter" and proposal of Ca. Fonsibacter lacus sp. nov. Syst Appl Microbiol. 2019;42:495–505.
21. Oh HM, Kang I, Lee K, Jang Y, Lim SI, Cho JC. Complete genome sequence of strain IMCC9063, belonging to SAR11 subgroup 3, isolated from the Arctic Ocean. J Bacteriol. 2011;193:3379–80.
22. Herlemann DPR, Woelk J, Labrenz M, Jürgens K. Diversity and abundance of "Pelagibacterales" (SAR11) in the Baltic Sea salinity gradient. Syst Appl Microbiol. 2014;37:601–4.
23. Henson MW, Lanclos VC, Pitre DM, Weckhorst JL, Lucchesi AM, Cheng C, et al. Expanding the diversity of bacterioplankton isolates and modeling isolation efficacy with large-scale dilution-to-extinction cultivation. Appl Environ Microbiol. 2020;86:e00943–20.
24. Rasmussen AN, Damashek J, Eloe-Fadrosh EA, Francis CA. In-depth spatio-temporal characterization of planktonic archaeal and bacterial communities in North and South San Francisco Bay. Microb Ecol. 2020. https://doi.org/10.1007/s00248-020-01621-7.
25. Brown MV, Fuhrman JA. Marine bacterial microdiversity as revealed by internal transcribed spacer analysis. Aquat Microb Ecol. 2005;41:15–23.
26. Schwalbach MS, Tripp HJ, Steindler L, Smith DP, Giovannoni SJ. The presence of the glycolysis operon in SAR11 genomes is positively correlated with ocean productivity. Environ Microbiol. 2010;12:490–500.
27. Malmstrom RR, Kiene RP, Cottrell MT, Kirchman DL. Contribution of SAR11 bacteria to dissolved dimethylsulfoniopropionate and amino acid uptake in the North Atlantic ocean. Appl Environ Microbiol. 2004;70:4129–35.
28. Tripp HJ, Kitner JB, Schwalbach MS, Dacey JWH, Wilhelm LJ, Giovannoni SJ. SAR11 marine bacteria require exogenous reduced sulphur for growth. Nature. 2008;452:741–4.
29. Smith DP, Nicora CD, Carini P, Lipton MS, Norbeck AD, Smith RD, et al. Proteome remodeling in response to sulfur limitation in "Candidatus Pelagibacter ubique.". mSystems. 2016;1:e00068–16.

30. Haro-Moreno JM, Rodriguez-Valera F, Rosselli R, Martinez-Hernandez F, Roda-Garcia JJ, Gomez ML, et al. Ecogenomics of the SAR11 clade. Environ Microbiol. 2019;22:1748–63.

31. Henson MW, Pitre DM, Weckhorst JL, Lanclos VC, Webber AT, Thrash JC. Artificial seawater media facilitate cultivating members of the microbial majority from the Gulf of Mexico. mSphere. 2016;1:1–10.

32. Bankevich A, Nurk S, Antipov D, Gurevich AA, Dvorkin M, Kulikov AS, et al. SPAdes: a new genome assembly algorithm and its applications to single-cell sequencing. J Comput Biol. 2012;19:455–77.

33. Walker BJ, Abeel T, Shea T, Priest M, Abouelliel A, Sakthikumar S, et al. Pilon: an integrated tool for comprehensive microbial variant detection and genome assembly improvement. PLoS One. 2014;9:e112963.

34. Parks DH, Imelfort M, Skennerton CT, Hugenholtz P, Tyson GW. CheckM: assessing the quality of microbial genomes recovered from isolates, single cells, and metagenomes. Genome Res. 2015;25:1043–55.

35. Rasmussen AN, Francis CA. Genome-resolved metagenomic insights into massive seasonal ammonia-oxidizing archaea blooms in San Francisco Bay. mSystems. 2022;7:e0127021.

36. Chaumeil P-A, Mussig AJ, Hugenholtz P, Parks DH. GTDB-Tk: a toolkit to classify genomes with the Genome Taxonomy Database. Bioinformatics. 2019;36:1925–7.

37. Edgar RC. MUSCLE: Multiple sequence alignment with high accuracy and high throughput. Nucleic Acids Res. 2004;32:1792–7.

38. Capella-Gutierrez S, Silla-Martinez JM, Gabaldon T. trimAl: a tool for automated alignment trimming in large-scale phylogenetic analyses. Bioinformatics. 2009;25:1972–3.

39. Nguyen L-T, Schmidt HA, von Haeseler A, Minh BQ. IQ-TREE: a fast and effective stochastic algorithm for estimating maximum-likelihood phylogenies. Mol Biol Evol. 2015;32:268–74.

40. Jain C, Rodriguez-R LM, Phillippy AM, Konstantinidis KT, Aluru S. High throughput ANI analysis of 90K prokaryotic genomes reveals clear species boundaries. Nat Commun. 2018;9:5114.

41. Eren AM, Esen ÖC, Quince C, Vineis JH, Morrison HG, Sogin ML, et al. Anvi'o: an advanced analysis and visualization platform for'omics data. PeerJ. 2015;3:e1319.

42. Eren AM, Kiefl E, Shaiber A, Veseli I, Miller SE, Schechter MS, et al. Community-led, integrated, reproducible multi-omics with anvi'o. Nat Microbiol. 2021;6:3–6.

43. Savoie ER, Lanclos VC, Henson MW, Cheng C, Getz EW, Barnes SJ, et al. Eco-physiology of the Cosmopolitan OM252 Bacterioplankton (Gammaproteobacteria). mSystems. 2021;6:e0027621.

44. Jones P, Binns D, Chang H-Y, Fraser M, Li W, McAnulla C, et al. InterProScan 5: genome-scale protein function classification. Bioinformatics. 2014;30:1236–40.

45. Roux S, Enault F, Hurwitz BL, Sullivan MB. VirSorter: mining viral signal from microbial genomic data. PeerJ. 2015;3:e985.

46. Alneberg J, Bennke C, Beier S, Bunse C, Quince C, Ininbergs K, et al. Ecosystem-wide metagenomic binning enables prediction of ecological niches from genomes. Commun Biol. 2020;3:119.

47. Alneberg J, Sundh J, Bennke C, Beier S, Lundin D, Hugerth LW, et al. BARM and BalticMicrobeDB, a reference metagenome and interface to meta-omic data for the Baltic Sea. Sci Data. 2018;5:180146.

48. Ahmed MA, Lim SJ, Campbell BJ. Metagenomes, metatranscriptomes, and metagenome-assembled genomes from Chesapeake and Delaware Bay (USA) water samples. Microbiol Resour Announc. 2021;10:e0026221.

49. Sakowski EG, Arora-Williams K, Tian F, Zayed AA, Zablocki O, Sullivan MB, et al. Interaction dynamics and virus-host range for estuarine actinophages captured by epicPCR. Nat Microbiol. 2021;6:630–42.

50. Fortunato CS, Crump BC. Microbial gene abundance and expression patterns across a river to ocean salinity gradient. PLoS One. 2015;10:e0140578.

51. Di Cesare A, Dzhembekova N, Cabello-Yeves PJ, Eckert EM, Slabakova V, Slabakova N, et al. Genomic comparison and spatial distribution of different Synechococcus phylotypes in the Black Sea. Front Microbiol. 2020;11:1979.

52. Thrash JC, Seitz KW, Baker BJ, Temperton B, Gillies LE, Rabalais NN, et al. Metabolic roles of uncultivated bacterioplankton lineages in the northern Gulf of Mexico "Dead Zone." MBio. 2017;8:e01017-17.

53. Xu B, Li F, Cai L, Zhang R, Fan L, Zhang C. A holistic genome dataset of bacteria, archaea and viruses of the Pearl River estuary. Sci Data. 2022;9:49.

54. Biller SJ, Berube PM, Dooley K, Williams M, Satinsky BM, Hackl T, et al. Marine microbial metagenomes sampled across space and time. Sci Data. 2018;5:180176.

55. Sunagawa S, Coelho LP, Chaffron S, Kultima JR, Labadie K, Salazar G, et al. Structure and function of the global ocean microbiome. Science. 2015;348:1261359.

56. Mende DR, Bryant JA, Aylward FO, Eppley JM, Nielsen T, Karl DM, et al. Environmental drivers of a microbial genomic transition zone in the ocean's interior. Nat Microbiol. 2017;2:1367–73.

57. Conner Y. Kojima, Eric W. Getz, and J. Cameron Thrash. RRAP: RPKM recruitment analysis pipeline. Microbiol Resour Announc. 2022; 11.

58. Cheng C, Thrash JC. sparse-growth-curve: A Computational Pipeline For Parsing Cellular Growth Curves With Low Temporal Resolution. Microbiol Resour Announc. 2021;10:e00296-21.

59. Konstantinidis KT, Tiedje JM. Towards a genome-based taxonomy for prokaryotes. J Bacteriol. 2005;187:6258–64.

60. Yarza P, Yilmaz P, Pruesse E, Glöckner FO, Ludwig W, Schleifer K-H, et al. Uniting the classification of cultured and uncultured bacteria and archaea using 16S rRNA gene sequences. Nat Rev Microbiol. 2014;12:635–45.

61. Battaglia B. Final resolution of the symposium on the classification of brackish waters. Archo Oceanogr Limnol. 1959;11:243–8.

62. Thrash JC, Boyd A, Huggett MJ, Grote J, Carini P, Yoder RJ, et al. Phylogenomic evidence for a common ancestor of mitochondria and the SAR11 clade. Sci Rep. 2011;1:13.

63. Ferla MP, Thrash JC, Giovannoni SJ, Patrick WM. New rRNA gene-based phylogenies of the Alphaproteobacteria provide perspective on major groups, mitochondrial ancestry and phylogenetic instability. PLoS One. 2013;8:e83383.

64. Viklund J, Martijn J, Ettema TJG, Andersson SGE. Comparative and phylogenomic evidence that the alphaproteobacterium HIMB59 is not a member of the oceanic SAR11 clade. PLoS One. 2013;8:e78858.

65. Martijn J, Vosseberg J, Guy L, Offre P, Ettema TJG. Deep mitochondrial origin outside the sampled alphaproteobacteria. Nature. 2018;557:101–5.

66. Muñoz-Gómez SA, Susko E, Williamson K, Eme L, Slamovits CH, Moreira D, et al. Site-and-branch-heterogeneous analyses of an expanded dataset favour mitochondria as sister to known Alphaproteobacteria. Nat Ecol Evol. 2022;6:253–62.

67. Kaczmarski JA, Hong N-S, Mukherjee B, Wey LT, Rourke L, Förster B, et al. Structural basis for the allosteric regulation of the SbtA bicarbonate transporter by the PII-like protein, SbtB, from cyanobium sp. PCC7001. Biochemistry. 2019;58:5030–9.

68. Alonso-Sáez L, Galand PE, Casamayor EO, Pedrós-Alió C, Bertilsson S. High bicarbonate assimilation in the dark by Arctic bacteria. ISME J. 2010;4:1581–90.

69. Sun J, Todd JD, Thrash JC, Qian Y, Qian MC, Temperton B, et al. The abundant marine bacterium Pelagibacter simultaneously catabolizes dimethylsulfoniopropionate to the gases dimethyl sulfide and methanethiol. Nat Microbiol. 2016;1:16065.

70. Veaudor T, Cassier-Chauvat C, Chauvat F. Genomics of urea transport and catabolism in cyanobacteria: biotechnological implications. Front Microbiol. 2019;10:2052.

71. Widner B, Fuchsman CA, Chang BX, Rocap G, Mulholland MR. Utilization of urea and cyanate in waters overlying and within the eastern tropical north Pacific oxygen deficient zone. FEMS Microbiol Ecol. 2018;94:1–15.

72. Sudesh K, Abe H, Doi Y. Synthesis, structure and properties of polyhydroxyalkanoates: biological polyesters. Prog Polym Sci. 2000;25:1503–55.

73. Obruca S, Sedlacek P, Koller M, Kucera D, Pernicova I. Involvement of polyhydroxyalkanoates in stress resistance of microbial cells: Biotechnological consequences and applications. Biotechnol Adv. 2018;36:856–70.

74. Oh S, Zhang R, Wu QL, Liu WT. Evolution and adaptation of SAR11 and Cyanobium in a saline Tibetan lake. Environ Microbiol Rep. 2016;8:595–604.

75. Campbell BJ, Lim SJ, Kirchman DL. Controls of SAR11 subclade abundance, diversity, and growth in two Mid-Atlantic estuaries. bioRxiv. 2022, https://www.biorxiv.org/content/10.1101/2022.05.04.490708v2.

76. Zubkov MV, Martin AP, Hartmann M, Grob C, Scanlan DJ. Dominant oceanic bacteria secure phosphate using a large extracellular buffer. Nat Commun. 2015;6:1–8.

77. Huang K, Wang D, Frederiksen RF, Rensing C, Olsen JE, Fresno AH. Investigation of the role of genes encoding zinc exporters zntA, zitB, and fieF during salmonella typhimurium infection. Front Microbiol. 2017;8:1–11.

78. Hopwood MJ, Statham PJ, Skrabal SA, Willey JD. Dissolved iron(II) ligands in river and estuarine water. Mar Chem. 2015;173:173–82.

79. Czech L, Hermann L, Stöveken N, Richter A, Höppner A, Smits S, et al. Role of the extremolytes ectoine and hydroxyectoine as stress protectants and nutrients: genetics, phylogenomics, biochemistry, and structural analysis. Genes. 2018;9:177.

80. Tao P, Li H, Yu Y, Gu J, Liu Y. Ectoine and 5-hydroxyectoine accumulation in the halophile Virgibacillus halodenitrificans PDB-F2 in response to salt stress. Appl Microbiol Biotechnol. 2016;100:6779–89.

81. Zhao X, Schwartz CL, Pierson J, Giovannoni SJ, McIntosh JR, Nicastro D. Three-dimensional structure of the ultraoligotrophic marine bacterium "Candidatus Pelagibacter ubique." Appl Environ Microbiol. 2017;83.

82. Giovannoni S, Stingl U. The importance of culturing bacterioplankton in the "omics" age. Nat Rev Microbiol. 2007;5:820–6.

83. Carini P, White AE, Campbell EO, Giovannoni SJ. Methane production by phosphate-starved SAR11 chemoheterotrophic marine bacteria. Nat Commun. 2014;5:1–7.

84. Suffridge CP, Bolaños LM, Bergauer K, Worden AZ, Morré J, Behrenfeld MJ, et al. Exploring vitamin B1 cycling and its connections to the microbial community in the north atlantic ocean. Front Marine Sci. 2020;7:1–16.

85. Patel MS, Nemeria NS, Furey W, Jordan F. The pyruvate dehydrogenase complexes: structure-based function and regulation. J Biol Chem. 2014;289: 16615–23.

86. Shikata H, Koyama S, Egi Y, Yamada K, Kawasaki T. Cytosolic adenylate kinase catalyzes the synthesis of thiamin triphosphate from thiamin diphosphate. Biochem Int. 1989;18:933–41.

87. Day JW Jr, Michael Kemp W, Yáñez-Arancibia A, Crump BC. Estuarine ecology. 2nd ed. Hoboken NJ: John Wiley & Sons; 2012.

88. Crump BC, Hopkinson CS, Sogin ML, Hobbie JE. Microbial biogeography along an estuarine salinity gradient: combined influences of bacterial growth and residence time. Appl Environ Microbiol. 2004;70:1494–505.

89. Herlemann DP, Labrenz M, Jürgens K, Bertilsson S, Waniek JJ, Andersson AF. Transitions in bacterial communities along the 2000 km salinity gradient of the Baltic Sea. ISME J. 2011;5:1571–9.

90. Logares R, Bråte J, Bertilsson S, Clasen JL, Shalchian-Tabrizi K, Rengefors K. Infrequent marine-freshwater transitions in the microbial world. Trends Microbiol. 2009;17:414–22.

91. Paver SF, Muratore D, Newton RJ, Coleman ML. Reevaluating the salty divide: phylogenetic specificity of transitions between marine and freshwater systems. mSystems. 2018;3:1–15.

92. Ramachandran A, McLatchie S, Walsh DA. A novel freshwater to marine evolutionary transition revealed within Methylophilaceae bacteria from the Arctic Ocean. MBio. 2021;12:e0130621.

93. Alverson AJ, Jansen RK, Theriot EC. Bridging the Rubicon: phylogenetic analysis reveals repeated colonizations of marine and fresh waters by thalassiosiroid diatoms. Mol Phylogenet Evol. 2007;45:193–210.

94. Luo H. Evolutionary origin of a streamlined marine bacterioplankton lineage. ISME J. 2015;9:1423–33.

95. Cottrell MT, Kirchman DL. Transcriptional control in marine copiotrophic and oligotrophic bacteria with streamlined genomes. Appl Environ Microbiol. 2016;82:6010–8.

96. Cabello-Yeves PJ, Picazo A, Camacho A, Callieri C, Rosselli R, Roda-Garcia JJ, et al. Ecological and genomic features of two widespread freshwater picocyanobacteria. Environ Microbiol. 2018;20:3757–71.

97. Konstantinidis KT, Tiedje JM. Prokaryotic taxonomy and phylogeny in the genomic era: advancements and challenges ahead. Curr Opin Microbiol. 2007;10:504–9.

AUTHOR CONTRIBUTIONS
VCL conducted data analysis, experimentation, generated the figures, and wrote the paper. ANR, CYK, and CC conducted data analysis and contributed to figures. MWH, BCF, and CAF contributed strains, data, and/or reagents. JCT devised the study, obtained funding, conducted data analysis, and assisted with manuscript preparation. All authors contributed edits to the final manuscript.

COMPETING INTERESTS
The authors declare no competing interests.

ADDITIONAL INFORMATION
Supplementary information The online version contains supplementary material available at https://doi.org/10.1038/s41396-023-01376-2.

Correspondence and requests for materials should be addressed to J. Cameron Thrash.

Reprints and permission information is available at http://www.nature.com/reprints

Publisher's note Springer Nature remains neutral with regard to jurisdictional claims in published maps and institutional affiliations.